

Failure Mode Analyses of Reinforced Concrete Beams Strengthened in Flexure with Externally Bonded Fiber-Reinforced Polymers

Henrik Thomsen¹; Enrico Spacone²; Suchart Limkatanyu³; and Guido Camata⁴

Abstract: As existing structures age or are required to meet the changing demands on our civil infrastructure, poststrengthening and retrofitting are inevitable. A relatively recent technique to strengthen reinforced concrete (RC) beams in flexure uses fiber-reinforced polymer (FRP) strips or sheets glued to the tension side of the beam. A number of researchers have reported that the failure mode of an FRP-strengthened RC beam can change from the desired ductile mode of an underreinforced beam to a brittle one. This paper analyzes the effects of this strengthening technique on the response and failure modes of a reference RC beam. A nonlinear RC beam element model with bond-slip between the concrete and the FRP plate is used to study how the failure mechanism of simply supported strengthened RC beams is affected by the following parameters: plate length, plate width, plate stiffness, and loading type. The beam geometry is kept constant. The parametric studies confirm the experimentally observed results according to which the most commonly observed failure modes due to loss of composite actions are affected by the plate geometric and material properties. In addition, distributed loads (difficult to apply in an experimental test) may not be as sensitive to plate debonding in the region of maximum bending moment as are beams subjected to point loads.

DOI: 10.1061/(ASCE)1090-0268(2004)8:2(123)

CE Database subject headings: Failure modes; Fiber reinforced plastics; Concrete, reinforced; Composite beams; Bond stress; Constitutive models; Numerical analysis.

Introduction

In the flexural strengthening of reinforced concrete (RC) beams with externally applied fiber-reinforced polymer (FRP) sheets or strips, it is essential to understand the effects that the FRP reinforcement has on the beam failure mode, especially for the development of rational design equations under ultimate loading conditions. The review of the published literature on experimental studies on the response of RC beams strengthened with externally bonded FRP reveals that several different failure modes, from ductile to very brittle, were observed. The list of failure modes is classified here into two types. Type 1 includes modes exhibiting composite action up to failure of the strengthened beam and type 2 includes modes where failure is due to the loss in composite action (also called debonding failure).

Type 1 Failures: Beams Exhibiting Composite Action up to Failure

Steel yielding followed by concrete crushing: The flexural strength of the beam is reached with yielding of the tensile steel reinforcement followed by crushing of the concrete in the compression zone, while the FRP is intact. This happens if both the original and the strengthened beams are underreinforced.

Concrete crushing before steel yielding: For very high reinforcement ratios, failure of the RC element may be caused by compressive crushing of the concrete before the tensile steel yields and before the FRP ruptures. This mode is brittle and undesirable. It indicates that: (1) flexural strengthening of an overreinforced RC beam may not be a viable solution; and (2) when dealing with an underreinforced RC beam, its strengthening should not make it overreinforced.

Steel yielding followed by FRP rupture: For relatively low ratios of both steel and FRP reinforcement, flexural failure may occur with yielding of the tensile steel reinforcement followed by tensile rupture of the FRP prior to crushing of the concrete. The FRP reinforcement must be well anchored for this failure to take place (Bonacci and Maalej 2001).

Shear failure: The RC beam may reach its shear limit prior to any kind of flexural failure if not properly reinforced in shear. This happens when the moment capacity of the beam has been increased by externally bonded FRP laminates to a point where the shear capacity of the beam is reached before the beam fails in flexure (Seim et al. 2001).

Steel yielding in section with no FRP: For beams strengthened with very short plates, steel yielding can progress to a point along the beam where there is no FRP and a crack has formed in the concrete, effectively forming a plastic hinge at the ends of the

¹Major, U.S. Army, United States Military Academy, West Point, NY 10996.

²Professor, Dept. PRICOS, Facolta' di Architettura, Univ. G. D'Annunzio di Chieti-Pescara, 65127 Pescara, Italy; Adjunct Professor, Dept. of CEAE, Univ. of Colorado, Boulder, CO 80309-0428.

³Lecturer, Dept. of Civil Engineering, Prince of Songkla Univ., Hadyai, Songkla, Thailand, 90110.

⁴Research Associate, Dept. of CEAE, Univ. of Colorado, Boulder, CO 80309-0428; Dept. PRICOS, Facolta' di Architettura, Univ. F D'Annunzio di Chieti-Pescara, Italy.

Note. Discussion open until September 1, 2004. Separate discussions must be submitted for individual papers. To extend the closing date by one month, a written request must be filed with the ASCE Managing Editor. The manuscript for this paper was submitted for review and possible publication on July 9, 2002; approved on October 7, 2002. This paper is part of the *Journal of Composites for Construction*, Vol. 8, No. 2, April 1, 2004. ©ASCE, ISSN 1090-0268/2004/2-123-131/\$18.00.

plate. Composite action between the FRP and the concrete has not been lost (Mayo et al. 2000; Seim et al. 2001).

Type 2 Failures: Beams Exhibiting Loss of Composite Action at Failure

End of plate peeling: Initiating at the end of the FRP plate, this failure mode is caused by the transfer of shear stresses from the FRP to the concrete. A layer of concrete is separated with the FRP. The amount of concrete that debonds has been reported at levels from a few millimeters to the entire concrete cover. The peak shear stresses are caused by the beam section geometric discontinuity at the plate end. This failure mode typically occurs in beams reinforced with plates that are short and is very brittle in nature (Tumialan et al. 1999; Fanning and Kelly 2001; Sebastian 2001; Seim et al. 2001).

Midspan debonding: Initiating at a flexural crack in the region of maximum bending moment near the concentrated load, this failure mode is also caused by the transfer of shear stresses from the FRP plate to the concrete. The peak shear stresses are caused by the gradient in the plate strain resulting from changes in the moment diagram adjacent to the concentrated load and the tensile steel reinforcement yielding. This failure mode is typically more ductile than the previous one, because the response of the beam is taken to a level where the tensile steel yields, allowing for greater deflections and ductility (Tumialan et al. 1999; Zarnic et al. 1999; Fanning and Kelly 2001; Sebastian 2001).

The failure mechanism exhibited by a given RC beam strengthened in flexure with FRP plates depends on several parameters, both geometric and mechanical. The failures modes due to loss of composite actions are the most commonly observed, yet they are not fully understood, mainly because of the large cost of repeated experimental tests. This paper presents the results of an analytical study on different parameters that may affect the failure modes involving loss of composite action. The analytical studies use nonlinear frame analysis techniques based on a two-node,

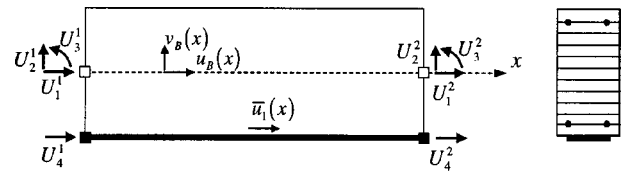


Fig. 2. Two-node displacement-based reinforced concrete beam element with bond-slip and layered section (Spacone and Limkatanyu 2000)

Euler-Bernoulli RC beam model with bond-slip that was developed to study the bond-slip effects between bars and concrete in RC structures. The parametric studies presented hereafter focus on how plate length, width, stiffness, and type of loading affect the failure mechanism of a reference underreinforced RC beam. Because the element used in the simulations does not consider shear deformations or shear failure, all applications deal with beams where shear failure of the RC beam was not an issue.

Parametric Studies on Fiber-Reinforced Polymer-Strengthened Reinforced Concrete Beams Loaded in Four-Point Bending

All the parametric studies presented in this paper use the same reference underreinforced shallow beam shown in Fig. 1. A similar beam was tested up to failure under four-point bending conditions at the University of Ljubljana, Slovenia (Zarnic et al. 1999). The analytical studies use a two-node displacement-based RC beam element with bond-slip between the plates and the concrete. The element formulation is presented in Spacone and Limkatanyu (2000), and the element is implemented in the general purpose finite-element program FEAP (Taylor 2002). The element is shown in Fig. 2. The element formulation uses classical cubic transverse displacements for the beam and linear axial displacements for the beam and the strengthening plate, resulting in a quadratic bond-slip distribution. The element uses a smeared crack representation of the concrete cracking in the elements. The concrete beam section is subdivided into layers, as shown in Fig. 2. Though more accurate mixed and forced-based elements are discussed by Limkatanyu and Spacone (2002), the simple two-node displacement-based element is used here because of its simplicity and ease of implementation. Aprile et al. (2001) use the same beam model to present a series of correlation studies between experimental and analytical results on RC beams strengthened with both steel and FRP plates.

The symmetry of the RC beam of Fig. 1 is taken advantage of by simulating only half of the beam. A fine mesh is used along the

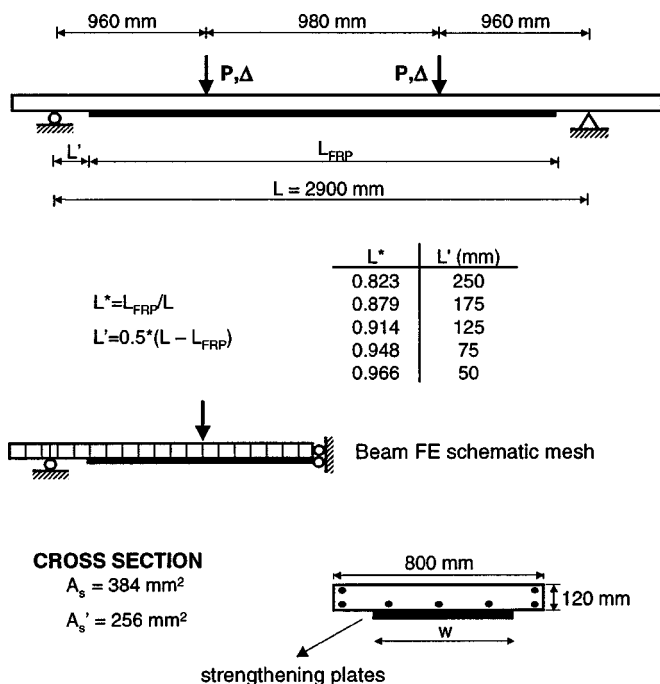


Fig. 1. Geometry and cross section of simulated RC beams

Table 1. Material Properties Used in Simulations

Material	Elastic modulus (GPa)	Compressive strength (MPa)	Tensile strength (MPa)
Concrete	27	25	1
Steel bars	210	460	460
Epoxy resin	12.8	—	4
Carbon fiber-reinforced polymer plate	140	—	1,800
Glass fiber-reinforced polymer plate	45	—	1,380

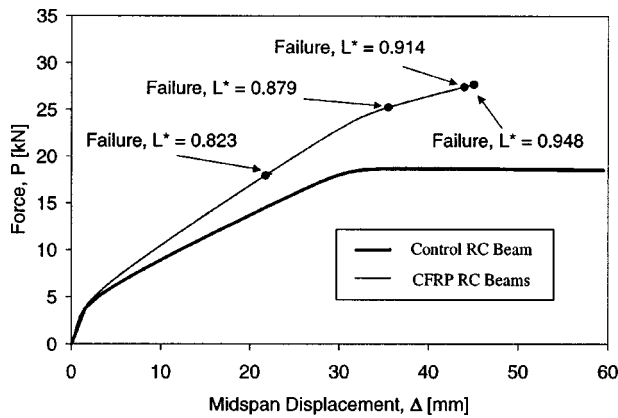


Fig. 3. Force-displacement response of reinforced concrete (RC) beams strengthened with carbon fiber-reinforced polymer (CFRP) plates of different length

beam of Fig. 1 in order to obtain accurate and detailed results. The material properties used for the parametric studies are summarized in Table 1. For the bond between the concrete and the reinforcing plate, a linear elastic bond law up until failure is used. The bond linear elastic properties are based on the actual elastic properties of the epoxy resin used for the connection, while the failure condition is mainly dependent on the concrete strength and surface preparation. Debonding failure in the beam is deemed to occur once the bond force limit is reached at any one location along the beam. According to the mechanical properties of the epoxy resin used in the experimental tests by Zarnic et al. (1999), a bond elastic shear stiffness of 2.384 GPa is assumed for the numerical simulations, while a value of 3.1 MPa is used for the bond strength. This bond strength, which is similar to the shear strength of the concrete, correlates well with the experimental results of Zarnic et al. (1999). Plate debonding is due not to epoxy failure, but to concrete shear failure at the concrete-epoxy interface, where a state of almost pure shear exists (Aprile et al. 2001). It is also assumed that the beam has sufficient stirrups to prevent premature shear failure. Finally, even though loss of composite action is the main focus of this study, other types of failures such as FRP tensile rupture and concrete crushing can be captured by the beam model used in the simulations.

Effect of Carbon Fiber-Reinforced Polymer Plate Length

The first series of parametric studies deals with the effect of the carbon fiber-reinforced polymer (CFRP) plate length. To distinguish between different plate lengths, a normalized plate length $L^* = L_{FRP}/L$ is introduced, where L = beam span and L_{FRP} = plate length, as shown in Fig. 1. L' indicates the distance from the beam support. The plates have a constant width $w = 100$ mm and a thickness of 1.2 mm for a plate area $A_{FRP} = 120$ mm². Zarnic et al. (1999) originally tested a similar beam with $L^* = 0.931$, or $L' = 100$ mm.

Fig. 3 shows the response of the beam of Fig. 1 for increasing values of L^* . Also shown is the response of the nonstrengthened, control RC beam. All of the RC beams follow the same equilibrium path, varying only in the point of failure, where bond failure occurs. Normalized lengths shorter than $L^* = 0.823$ are not considered because they lead to no load capacity increase with respect to the nonstrengthened RC beam. Fig. 4 shows the relationship between the increase in ultimate load and the plate length.

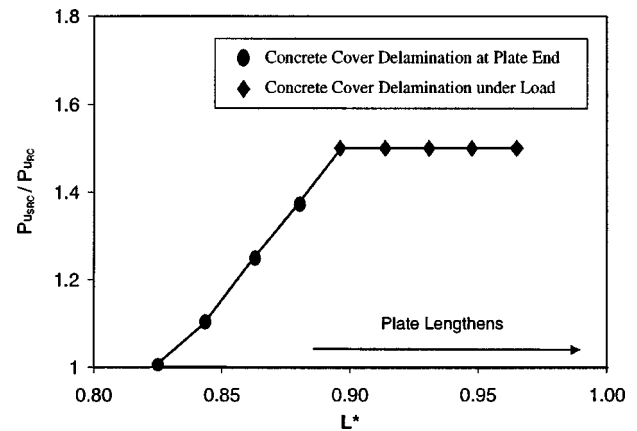


Fig. 4. Ultimate load increase for reinforced concrete (RC) beams with carbon fiber-reinforced polymer plates of different length

Pu_{SRC}/Pu_{RC} represents the ratio between the ultimate load Pu_{SRC} of the strengthened beam and the ultimate load Pu_{RC} of the nonstrengthened beam. A number of trends can be detected in these graphs. First, as the plate length increases, the ultimate load that the beam can carry increases. Second, the location of debonding (or concrete cover delamination) changes from plate end (end peeling) to midspan (midspan debonding) as the plate length increases. Finally, these results indicate that a certain effective length exists, beyond which an increase in plate length does not cause a noticeable increase in ultimate load. In other words, if the plate is sufficiently anchored, the beam fails due to delamination under the load and no increase in strength is obtained. The original experiment by Zarnic et al. (1999) had a plate with $L^* = 0.931$ and failed due to midspan debonding, in agreement with the results of Fig. 4.

To examine the trends observed in Figs. 3 and 4, the concrete-FRP interface bond force at the step prior to failure is examined. Fig. 5 shows the bond force distributions for a representative number of plate lengths. The plate ends and the loaded point show spikes in the bond force. The bond force is essentially the derivative of the plate force, and at these locations, the plate force slope has large discontinuities. The discontinuity at the plate end is caused by the change in beam cross section, with the plate force jumping from zero at the plate end section to an almost constant

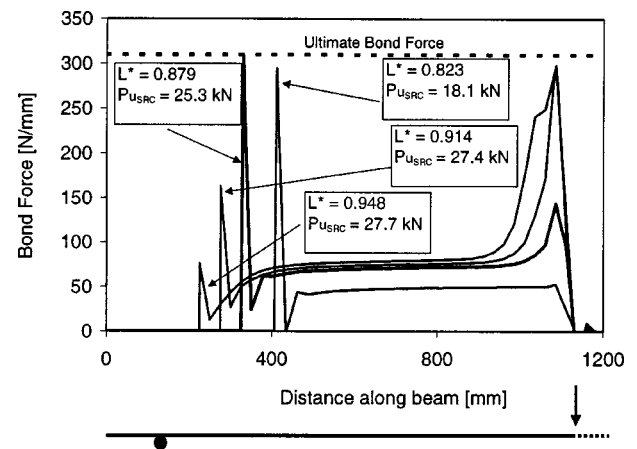


Fig. 5. Bond force distribution at failure for reinforced concrete beams strengthened with carbon fiber-reinforced polymer plates of different length

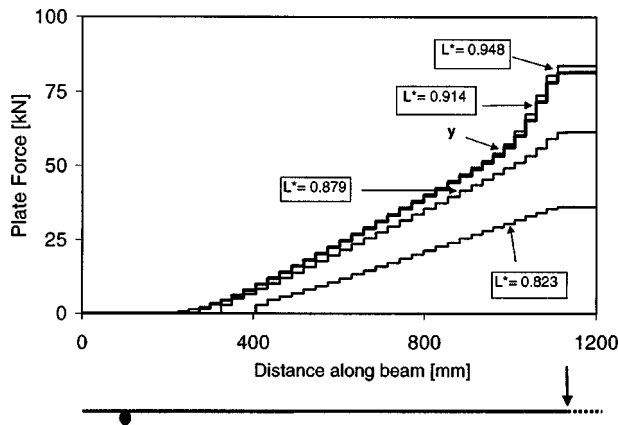


Fig. 6. Plate force distribution at failure for reinforced concrete beams strengthened with carbon fiber-reinforced polymer plates of different length

value in the composite section after a certain length. Under the point load, the plate force increases rapidly because the plate carries much more of the tensile force after the reinforcing steel yields in the area of maximum moment. Fig. 6 complements Fig. 5 by showing the distribution of the plate force. The steel yield penetration from midspan arrives at point *y*, at which the plate force changes slope because the FRP has to carry any increase in tension once the steel yields. Fig. 5 also confirms that, as the plate length decreases, the location along the beam where the bond failure occurs switches from under the load to the plate end. Shorter plates imply large bond stress jumps only at the plate end, because the steel does not yield under the load, while longer plates allow the beam to carry a larger load and the steel reinforcement can yield under the load, thus causing large bond forces that eventually cause bond failure.

An important issue in the strengthening of RC beams with FRP plates is the loss in ductility of the strengthened beams. Fig. 7 schematically shows the response of a strengthened RC beam. Point A corresponds to first concrete cracking, point B to first steel yielding, and point C to failure. Two definitions of ductility are used by Thomsen (2002), one displacement-based, the other energy-based. Because both definitions lead to the same conclu-

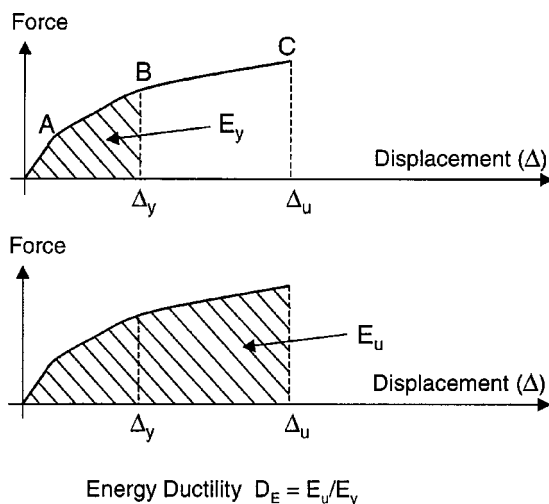


Fig. 7. Definition of energy ductility

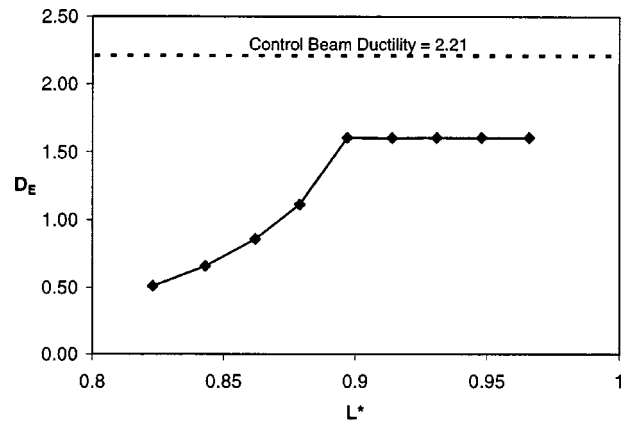


Fig. 8. Energy ductility for reinforced concrete beams strengthened with carbon fiber-reinforced polymer plates of different length

sions, only the energy-based ductility is used here. The energy ductility D_E is defined as the ratio between the energy of the system at failure E_u and the energy of the system at first steel yield E_y ; that is

$$D_E = \frac{E_u}{E_y} \quad (1)$$

Fig. 8 shows how the energy ductility changes as the strengthening plate lengthens. As expected, the overall ductility of the beam strengthened with an FRP plate is lower than that of the control RC beam. Also, longer plates generally lead to higher ductility, with a threshold length (basically the anchorage length, which for the present beam and plate geometry is approximately $L^* = 0.9$) beyond which no significant increase ductility is observed. For very short plates, the ductility is actually smaller than 1, indicating that delamination takes place before the reinforcing bars yield, as already noted in Figs. 5 and 6. It should be pointed out that these trends are peculiar to the RC beam geometry used in these studies. Further parametric studies are needed to investigate how the plate length affects RC beams of different geometries and reinforcement.

Effect of Carbon Fiber-Reinforced Polymer Plate Width

As seen in the previous section, bond stresses at the FRP-concrete interface play a central role in the failure of RC beams strengthened with externally bonded FRP. The bond stresses are directly influenced by the contact area between the FRP and concrete. As the contact area is increased, for a given load the bond stress should decrease. The simplest way to change the contact area between the concrete and the FRP is to introduce FRP plates with varying width w . The area A_{FRP} of the CFRP plate of Fig. 1 is kept constant while the width and thickness were adjusted. The plate length is kept constant at $L^* = 0.966$, which represents a plate that ends 50 mm from the support. Full anchorage is ensured by this width.

Fig. 9 shows the response of the RC beam with CFRP plates of varying widths and constant area, while Fig. 10 shows the increase in ultimate load by plotting the ultimate force ratio Pu_{SRC}/Pu_{RC} . As expected, the ultimate load increases with the plate width. Little strength increase is observed for widths of 50 and 75 mm. This is because, in this width range, the bottom steel does not yield before failure takes place for midspan debonding. The FRP plate does not carry much load until the steel yields,

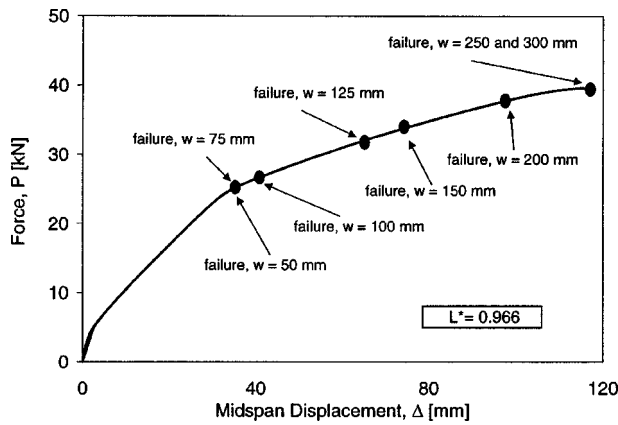


Fig. 9. Force-displacement response of reinforced concrete beams strengthened with carbon fiber-reinforced polymer plates of different width ($L^* = 0.966$)

thus the small increase in load-carrying capacity for the two widths. A larger load increase is observed for a width of 100 mm, because the bottom reinforcement has yielded at failure. No strength increase is observed for plates wider than 250 mm, because for wider plates, the beam failure mode switches from concrete cover delamination to FRP rupture. With the increased plate width, the FRP-concrete contact area is increased, distributing the bond stress over a larger area and thus allowing for a higher bond force to build before failure, as shown in Fig. 11. This leads to higher ultimate loads, as long as other failure mechanisms do not intervene (as is the case for plates wider than 250 mm). Fig. 12 shows the bond stress distribution along the FRP-concrete interface. Except for the beam with a plate width of 300 mm, all beams reached the maximum bond stress under the load. As stated earlier, for the 300-mm-wide plate, the FRP ruptured before the ultimate bond stress was reached. Fig. 12 also shows the larger penetration of steel yielding in the beams with a wider plate. This is particularly evident in the different shapes of the bond stress distributions for $w = 75$ mm and $w = 150$ mm. For $w = 75$ mm, the bond stress is almost constant away from the point load application. There is no yield penetration. On the other hand, for $w = 150$ mm, the yield penetration region extends to about 900 mm from the left end of the beam, as shown by the large bond stresses in the plateau to the left of the point of load application.

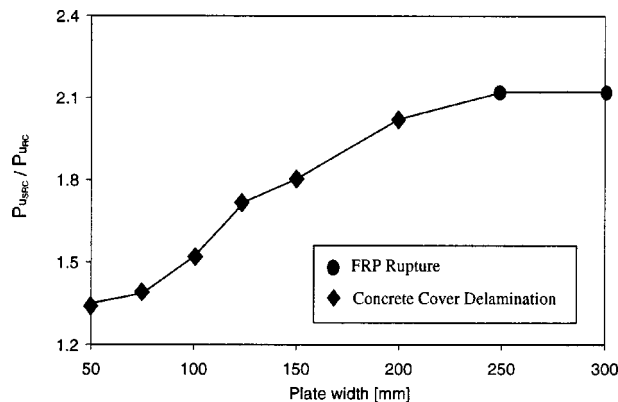


Fig. 10. Increase in ultimate load for reinforced concrete beams reinforced with carbon fiber-reinforced polymer (CFRP) plates of different width ($L^* = 0.966$)

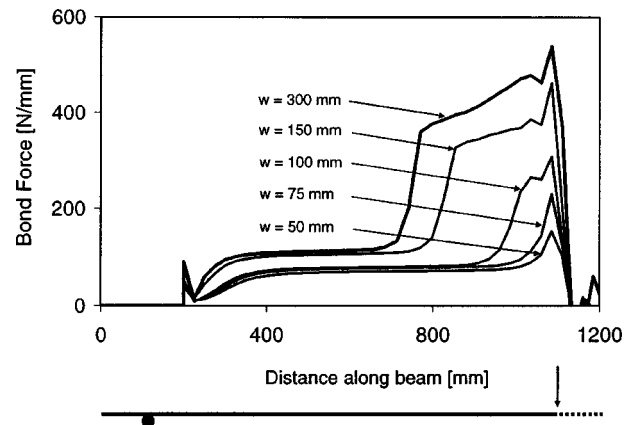


Fig. 11. Bond force distribution at failure for reinforced concrete beams strengthened with carbon fiber-reinforced polymer plates of different width ($L^* = 0.966$)

Because the steel yield penetration is greater when wider plates are used, the response is also more ductile. The energy ductility for different plate widths is shown in Fig. 13. Increasing the plate width also increases the beam ductility, and for large widths the ductility of the strengthened beam is much larger than that of the control beam. There is not much ductility increase for w larger than 250 mm, because for larger widths the FRP plates rupture before delamination takes place. The failure mode of the 300-mm-wide plate is an ideal one, because it shows large ductility and full use of the FRP plate. Larger widths thus lead to more cost-effective strengthening (Arduini and Nanni 1997). It should, however, be added that larger plates prevent concrete breathing, and this issue needs to be further investigated.

Response Comparison for Beams Strengthened with Glass Fiber-Reinforced Polymer and Carbon Fiber-Reinforced Polymer

The most widely used and studied composites for flexural strengthening of RC beams are carbon FRPs. The stiffness, strength, and time-dependent properties of CFRPs lend themselves well to the repair and strengthening of RC beams. The use of glass FRPs (GFRP) has also been studied. GFRPs are attractive

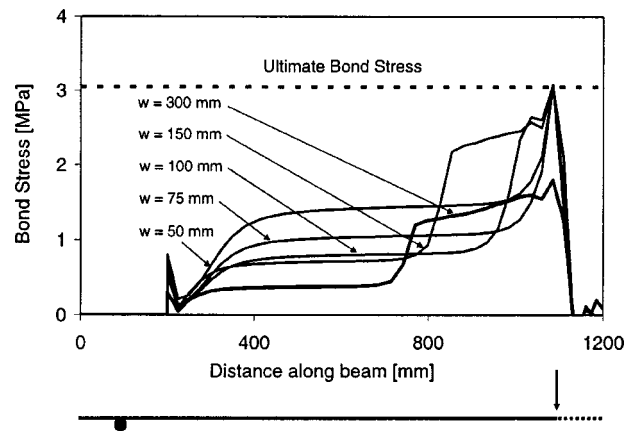


Fig. 12. Bond stress distribution at failure for reinforced concrete beams strengthened with carbon fiber-reinforced polymer plates of different width ($L^* = 0.966$)

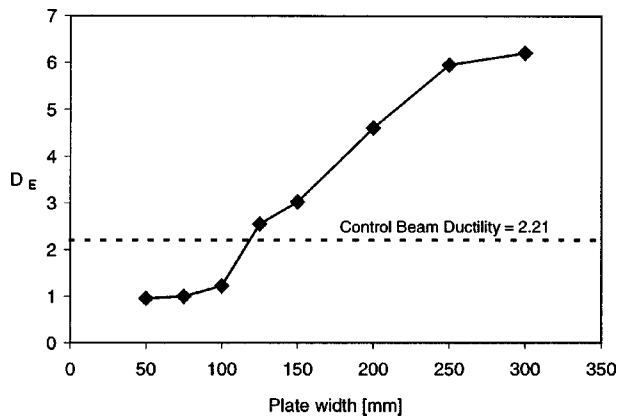


Fig. 13. Energy ductility of reinforced concrete beam strengthened with carbon fiber-reinforced polymer plates of different width

because of their low cost and high ultimate strain. Though more GFRP material would generally be needed to achieve the same overall axial strength, the cost difference can be large enough to make GFRP more efficient. The main drawback of GFRPs is their long-term performance. GFRP materials subjected to a constant load over time can fail suddenly after a certain time period, referred to as endurance time. This failure is known as creep rupture. Of the three most widely used fibers (carbon, glass, and aramid), glass is the most susceptible to creep rupture. To avoid this type of failure, the American Concrete Institute (2000) recommends keeping the material at less than 20% of its maximum stress value for sustained service loads. Finally, GFRP is more sensitive to environmental conditions.

To compare the behavior of beams strengthened in flexure with externally bonded plates of the two materials, CFRP and GFRP, a new set of four-point bending analyses is repeated using GFRP plates. The same reinforcement index is selected for CFRP and GFRP strengthening, thus leading to the same axial strength for the GFRP and CFRP plates. The values of the plate stiffness and ultimate stresses are selected based on the values typically provided by the manufacturers and available from the published literature. Table 1 contains the CFRP and GFRP plate properties. Because the ultimate stress of the GFRP used is lower than that of the CFRP plate, an area of GFRP 1.3 times that of the CFRP is

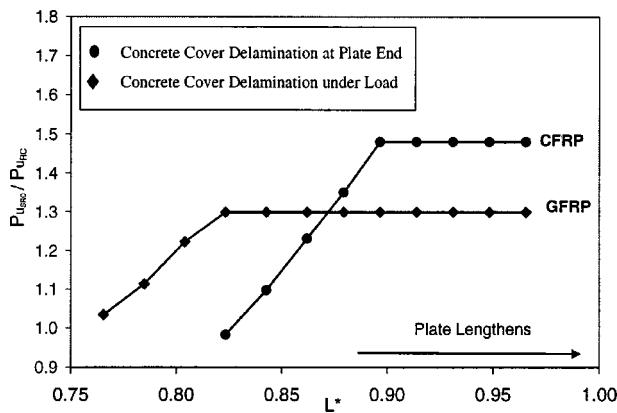


Fig. 14. Ultimate load increase over control beam under four point bending for reinforced concrete beams strengthened with glass fiber-reinforced polymer (GFRP) and carbon fiber-reinforced polymer (CFRP) plates of different length

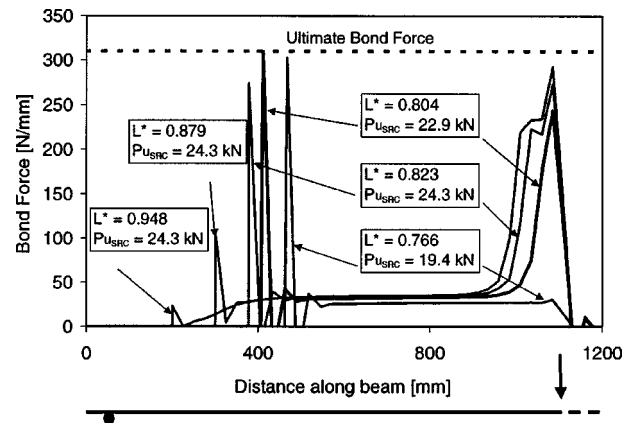


Fig. 15. Bond force distribution at failure for a glass fiber-reinforced polymer-strengthened reinforced concrete beam under four point bending

needed to achieve the same strength. The plate width is kept at $w = 100$ mm, with a different thickness in the CFRP and GFRP plates. The resulting axial stiffness of the GFRP plate is about 40% more than that of the CFRP plate.

Fig. 14 shows the ultimate load increase $P_{U,SRC}/P_{U,RC}$ over the control beam for beams strengthened with CFRP and GFRP plates of different length. These plots show that, given a plate long enough to avoid end peeling, CFRP provides a greater strength increase if the same reinforcing index is used. However, Fig. 14 also shows that end peeling occurs on longer plates for CFRP-strengthened beams than it does in GFRP-strengthened beams. In other words, the more flexible GFRP plates need shorter anchorage lengths. The reason for this difference can be analyzed by comparing the bond force distributions at failure for beams strengthened with the two materials. Fig. 15 shows the bond force distribution at failure for beams strengthened with GFRP plates of various lengths and should be compared with the bond stresses of CFRP-strengthened beams shown in Fig. 5. As the GFRP plate length decreases, the bond failure point for the GFRP-plated beam switches from under the load to the plate end at a length of approximately $L^* = 0.8$. This is compared with an anchorage length of about $L^* = 0.9$ for the CFRP-plated beam. Due to its greater axial stiffness, the CFRP plate requires a greater length to

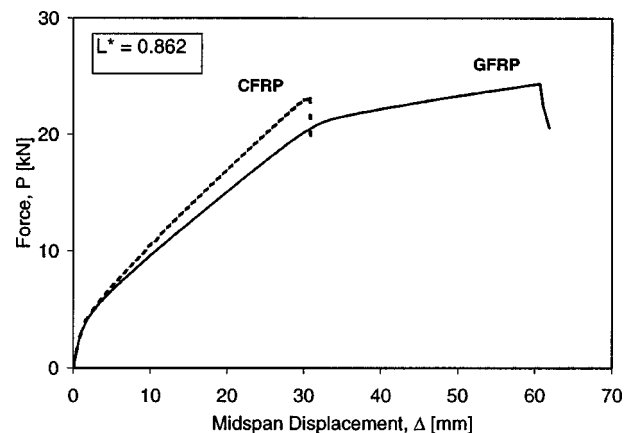


Fig. 16. Force-displacement response of reinforced concrete beams reinforced with glass fiber-reinforced polymer (GFRP) and carbon fiber-reinforced polymer (CFRP) plates ($L^* = 0.862$)

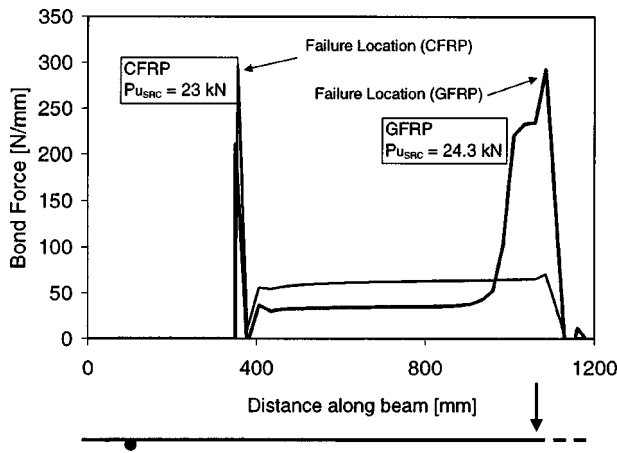


Fig. 17. Bond force distribution for reinforced concrete beams strengthened with carbon fiber-reinforced polymer (CFRP) and glass fiber-reinforced polymer (GFRP) ($L^* = 0.862$)

avoid end peeling. If, at the limit, an infinitely rigid plate were used, no bond-stress would develop (there would be constant stress in the plate) and all the bond-stress would concentrate at the plate end, thus leading to very early debonding. Of course, the stiffness of the plates used in the simulations are not of such extreme properties, but the analogy helps illustrate the reason for increased bond stresses in the stiffer CFRP plate end as compared with the GFRP plate.

To further study the reason for this difference in response, the comparison of a beam with CFRP and GFRP plates of equal length $L^* = 0.862$ is presented. This length is selected because of the different failure modes it produces for the GFRP and CFRP-plated beams. The GFRP-strengthened beam failed under the point load, while the CFRP-strengthened beam failed at the plate end. Fig. 16 shows the force-displacement response of the two beams. The responses are quite similar until the point of first concrete cracking. After cracking, the CFRP-plated beam has a stiffer response. Both beams fail at approximately the same load, but the GFRP-plated beam displacement and ductility at failure are much larger. This more ductile response is due to the fact that, for the GFRP-plated beam, the steel reinforcement is allowed to yield long before failure of the beam. Fig. 17 shows the bond force distribution at failure for both beams. The difference in

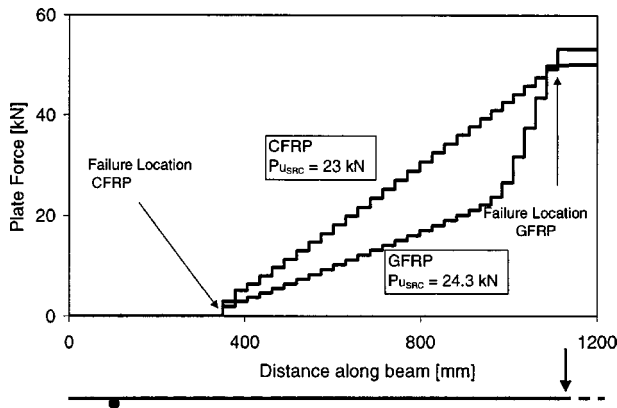


Fig. 18. Plate force distribution for reinforced concrete beams strengthened with glass fiber-reinforced polymer (GFRP) and carbon fiber-reinforced polymer (CFRP) ($L^* = 0.862$)

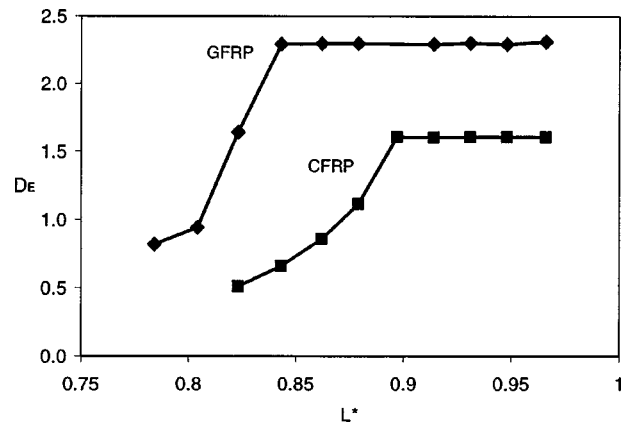


Fig. 19. Energy ductility for reinforced concrete beams strengthened with plates of different length and material

location of bond force failure can clearly be seen. Fig. 18 shows the plate force distribution for both beams at failure. The change in slope in the GFRP plate force indicates the penetration of steel reinforcement yielding along the beam. As for the ductility of the system, it is also largely influenced by the stiffness of the strengthening FRP plate. Fig. 19 shows the beam energy ductility for different plate lengths for both strengthening types. The more flexible GFRP plates lead to a more ductile response.

Reinforced Concrete Beams Strengthened in Flexure with Carbon Fiber-Reinforced Polymer Plates Subject to Distributed Loads

While all specimens experimentally tested and reviewed in the published literature were loaded under three- or four-point load conditions, several beams are subjected to mostly distributed loads. Concentrated loads may better describe the loads on bridge girders, while distributed loads better simulate the loading of beams in RC buildings. Due to the difficulty in testing beams under distributed loads, the strengthening or repair with FRP materials of RC beams under distributed loads has received little attention in the published literature.

To study the effect that the change in loading scheme has on the failure modes of FRP-strengthened RC beams, the response of

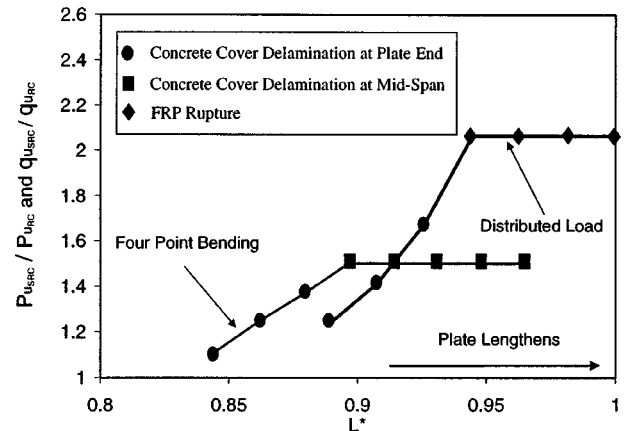


Fig. 20. Ultimate load increase for reinforced concrete beams strengthened with carbon fiber-reinforced polymer (CFRP) plates of different length

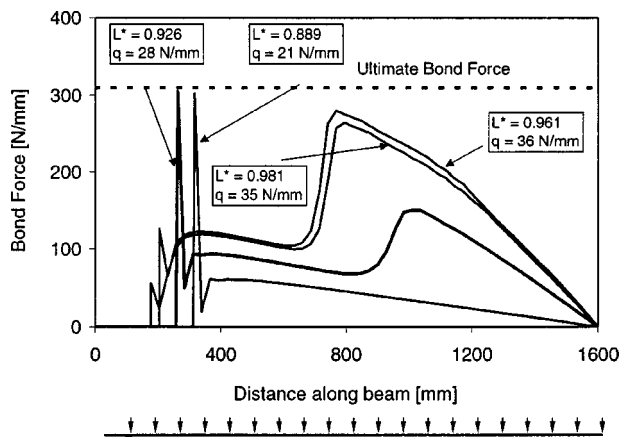


Fig. 21. Bond force distribution at failure for reinforced concrete beams with carbon fiber-reinforced polymer plates of different length under distributed load

the beam in Fig. 1 strengthened with CFRP plates of different lengths is simulated under an increasing distributed load q . A pattern similar to that of the four-point bending case can be seen in Fig. 20 for the beams under distributed load; the ultimate load increase begins to drop as the plate length shortens beyond a certain value. Fig. 20 plots both Pu_{SRC}/Pu_{RC} for the four-point bending loading scheme and qu_{SRC}/qu_{RC} for the beams under distributed load, where qu_{SRC} =ultimate distributed load for the strengthened beam, and qu_{RC} =ultimate distributed load for the nonstrengthened beam. Two main differences are evident. First, for relatively long plates ($L^* > 0.91$), the overall ultimate load increase is greater for the distributed load case. Second, the failure mode observed in beams strengthened with longer, well-anchored plates is not midspan debonding as in the four-point bending case, but FRP rupture.

The reason for these trends in the beam failure modes is apparent in Fig. 21, which shows the bond force distribution at failure for RC beams strengthened with CFRP plates of different lengths. The bond force is plotted for half of the beam. The beams strengthened with longer plates, in this case $L^* = 0.961$ and $L^* = 0.981$, are allowed to develop their maximum plate force, because there is no bond force discontinuity under the load. In the absence of concentrated loads, the plate force slope is continuous

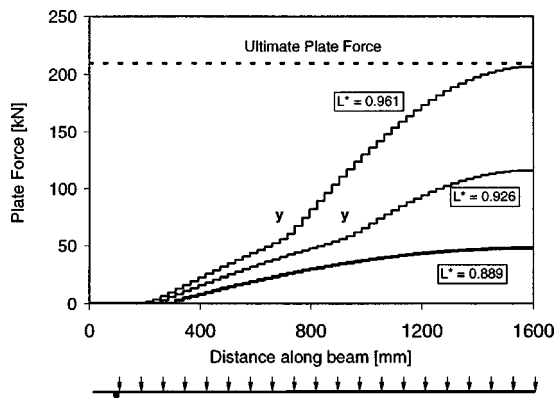


Fig. 22. Plate force distribution at failure for reinforced concrete beams with carbon fiber-reinforced polymer plates of different length subjected to a distributed load

under the load. The sudden drop on bond force for $L^* = 0.961$ and $L^* = 0.981$ at roughly 700 mm along the beam corresponds to the transition between yielded steel (to the right) and elastic steel (to the left). Fig. 22 shows the plate force distributions. As in the four-point bending case, the point along the beam to which the reinforcing steel yield penetrates can be identified by the change in slope of the plate force (labeled as point “y”). In the four-point bending case, the presence of a concentrated load creates a large discontinuity in the plate force derivative, which is proportional to the bond force at that point. Because the distributed load causes no discontinuity under the load apart from the discontinuity at the plate end, the bond force does not peak in the area of maximum moment. Fig. 22 shows that for $L^* = 0.961$ (the case with $L^* = 0.981$ is omitted because it gives basically identical results) the plate force reaches its ultimate strength (FRP rupture). As the plate shortens, the failure mode of end peeling develops due to the high stress concentrations of the plate end. It should be noted that if, well-anchored GFRP plates with the same axial stiffness EA of the CFRP plates were used, higher ultimate loads and deflections would be reached because of the larger ultimate strain in the GRFP fibers (provided concrete does not crush before FRP rupture).

Summary and Conclusions

This paper applies a recently developed RC beam element with bond-slip between the concrete and the strengthening plate to the study of the failure mechanisms of RC beams strengthened in flexure with externally bonded FRPs. The focus of the paper is on the failure modes that occur because of the loss of composite action between the FRP and the concrete. The following conclusions can be drawn from the study:

- As already evidenced by experimental studies, the FRP plate length plays a significant role in the failure mode of strengthened RC beams. For beams loaded by point loads, there is a certain plate length that marks the threshold between debonding under the point load (for longer plates) and plate-end peeling (for shorter plates). The change in failure mode is due to the large bond-stress values (which translate into large concrete shear stresses) at the plate end and under the point loads. In short FRP plates, the peak bond stress is at the plate end, while longer FRP plates allow steel yielding to penetrate, thus causing larger bond stresses under the point loads. For the beam configuration considered in this study, no significant difference in load capacity is noted in beams that fail for plate-end peeling, indicating the existence of a plate “anchorage length.” For the reference narrow plate used in the first part of the study ($w = 100$ mm) the energy ductility of the strengthened beam is lower than that of the nonstrengthened beam. The energy ductility increases with the plate length until the failure mode shifts to midspan debonding, with no increase in ductility for longer plates.
- The FRP plate width influences the failure mode of the strengthened beams. Wider plates of equal cross section tend to reduce the bond stress at the concrete-FRP interface, allowing a more efficient use of the FRP plate strength and leading to higher ultimate beam flexural strengths. For the plate length considered in the examples, very large plates show a change in failure mode from midspan debonding to FRP plate rupture, because wider plates induce higher plate stresses. The energy ductility increases with wider plates and can be higher than that of the nonstrengthened beam.

- FRP plate stiffness significantly affects the strengthened beam response and failure mode. A comparison of beams strengthened in flexure with plates of different axial stiffness (CFRP and GFRP) and equal reinforcing index shows that the more flexible plates (GFRP) tend to have lower interface shear stresses at the plate end, thus needing a shorter anchorage length. If the plate is long enough to avoid plate-end peeling, the stiffer CFRP-plated beams show higher ultimate loads than the GFRP-plated beams. The energy ductility of GFRP-strengthened beams is higher than that of CFRP-strengthened beams of equal reinforcing index.
- FRP-strengthened RC beams tend to perform better under distributed loads than under four-point bending loading conditions. The distributed load does not cause a discontinuity in the plate force along the span. In the four-point bending case, the discontinuity caused by the concentrated load tended to cause midspan debonding. Shorter plates in the distributed load case exhibit a similar failure mode to that of four-point bending, with plate-end peeling due to the geometric discontinuity in the section. RC beams with longer plates eventually fail due to plate failure, as the plate can develop its full strength before bond failure. While concentrated loads may simulate bridge girders, distributed loads better simulate beams in RC buildings. GFRP may be a better choice for beams under distributed loads in RC buildings because of the higher plate protection against environmental factors and the GFRP higher ultimate strain, which can produce even higher beam strength and ductility.
- The RC beam element used in this study is quite simple and easy to implement. However, it allows performance of a number of parametric studies in a very short time. The element is a very useful tool to perform parametric studies that can complement past and ongoing experimental studies for the development of rational design equations.

Acknowledgments

This study was supported by the United States Army and its advanced civil schooling program, by the Royal Thai Fellowship, and by Grant No. CMS-9804613 from the National Science Foundation. This support is gratefully acknowledged. Any opinions expressed in this paper are those of the writers and do not reflect the views of the sponsoring agencies.

Notation

The following symbols are used in this paper:

D_E = energy ductility;

E_y, E_u = energy at first steel yielding and at beam failure;
 L, L_{FRP} = beam and plate length, respectively;
 L^* = normalized plate length;
 q = distributed load; and
 w = plate width.

References

- American Concrete Institute (ACI). (2000). *Guide for the design and construction of externally bonded FRP systems for strengthening concrete structures*, Detroit.
- Aprile, A., Spacone, E., and Limkatanyu, S. (2001). "Role of bond in beams strengthened with steel and FRP plates." *J. Struct. Eng.*, 127(12), 1445–1452.
- Arduini, M., and Nanni, A. (1997). "Parametric study of beams with externally bonded FRP reinforcement." *ACI Struct. J.*, 94(5), 493–501.
- Bonacci, J. F., and Maalej, M. (2001). "Behavioral trends of RC beams strengthened with externally bonded FRP." *J. Compos. Constr.*, 5(2), 102–113.
- Fanning, P., and Kelly, O. (2001). "Ultimate response of RC beams strengthened with CFRP plates." *J. Compos. Constr.*, 5(2), 122–127.
- Limkatanyu, S., and Spacone, E. (2002). "Reinforced concrete frame element with bond interfaces. I: Displacement-based, force-based, and mixed formulations." *J. Struct. Eng.*, 128(3), 346–355.
- Mayo, R., Nanni, A., Watkins, S., Barker, M., and Boothby, M. (2000). "Strengthening of bridge G-270 with externally bonded CFRP sheets." *Technical Rep. R198-012*, Missouri Dept. of Transportation, Springfield, Mo.
- Sebastian, W. (2001). "Significance of midspan debonding failure in FRP-plated concrete beams." *J. Struct. Eng.*, 127(7), 792–798.
- Seim, W., Hörmann, M., Karbhari, V., and Seible, F. (2001). "External FRP poststrengthening of scaled concrete slabs." *J. Compos. Constr.*, 5(2), 67–75.
- Spacone, E., and Limkatanyu, S. (2000). "Response of reinforced concrete members including bond-slip effects." *ACI Struct. J.*, 97(6), 831–839.
- Taylor, R. (2002). *FEAP: A finite element analysis program; users manual: version 7.4*, Dept. of Civil and Environmental Engineering, Univ. of California, Berkeley, Calif.
- Thomsen, H. H. (2002). "Failure mode analysis of reinforced concrete beams strengthened in flexure with externally bonded fiber reinforced polymers." MS thesis, Dept. of Civil, Environmental, and Architectural Engineering, Univ. of Colorado, Boulder, Colo.
- Tumialan, G., Serra, P., Nanni, A., and Belarbi, A. (1999). "Concrete cover delamination in RC beams strengthened with FRP sheets." *Proc., 4th Int. Symp. on FRP for Reinforcement of Concrete Structures*, American Concrete Institute, Detroit, 725–735.
- Zarnic, R., Gostic, S., Bosiljkov, V., and Bokan, V. (1999). "Improvement of bending load-bearing capacity by externally bonded plates." *Proc., Creating with Concrete*, R. K. Dhir and N. A. Henderson, eds., Thomas Telford, London, 433–442.